Photosynthesis Research (2023) 156:247–264
https://doi.org/10.1007/s11120-023-01000-6

RESEARCH

The carbon-concentrating mechanism of the extremophilic red microalga *Cyanidioschyzon merolae*

Anne K. Steensma[1,2] · **Yair Shachar-Hill**[1] · **Berkley J. Walker**[1,2]

Received: 25 November 2022 / Accepted: 27 January 2023 / Published online: 13 February 2023

Abstract

Cyanidioschyzon merolae is an extremophilic red microalga which grows in low-pH, high-temperature environments. The basis of *C. merolae*'s environmental resilience is not fully characterized, including whether this alga uses a carbon-concentrating mechanism (CCM). To determine if *C. merolae* uses a CCM, we measured CO_2 uptake parameters using an open-path infra-red gas analyzer and compared them to values expected in the absence of a CCM. These measurements and analysis indicated that *C. merolae* had the gas-exchange characteristics of a CCM-operating organism: low CO_2 compensation point, high affinity for external CO_2, and minimized rubisco oxygenation. The biomass $\delta^{13}C$ of *C. merolae* was also consistent with a CCM. The apparent presence of a CCM in *C. merolae* suggests the use of an unusual mechanism for carbon concentration, as *C. merolae* is thought to lack a pyrenoid and gas-exchange measurements indicated that *C. merolae* primarily takes up inorganic carbon as carbon dioxide, rather than bicarbonate. We use homology to known CCM components to propose a model of a pH-gradient-based CCM, and we discuss how this CCM can be further investigated.

Keywords Carbon-concentrating mechanisms · *Cyanidioschyzon merolae* · Cyanidiales · Photosynthesis · Extremophiles · Gas-exchange

Introduction

Phototrophs have an array of strategies to combat photosynthetic inefficiencies that arise from the competition between carbon dioxide (CO_2) and molecular oxygen (O_2) fixation by rubisco (EC 4.1.1.39), the initial enzyme of C_3 photosynthesis. Some photosynthetic organisms are capable of increasing CO_2 fixation efficiency by operating carbon-concentrating mechanisms (CCMs), which help inhibit rubisco's oxygenase activity by increasing the CO_2 concentration around rubisco. Aquatic organisms are notable for their widespread and varied CCMs, which enable them to be highly photosynthetically productive despite the limited solubility and slow diffusion of CO_2 in aqueous environments (Griffiths et al. 2017). In particular, aquatic organisms with CCMs predominately operate various biophysical CCMs, which are CCMs that involve movement of dissolved inorganic carbon (DIC) species, rather than involving the fluxes of carbon through organic carbon metabolism which characterize the biochemical CCMs of C_4 and CAM plants (Barrett et al. 2021). Expanding our knowledge of this CCM diversity is essential to understanding how organisms resist environmental challenges and may reveal new approaches to overcoming biotechnological challenges. For example, the engineering of aquatic CCMs into C_3 crop plants represents a possible avenue for increasing agricultural productivity (Price et al. 2011; McGrath and Long 2014; Meyer et al. 2016; Rae et al. 2017; Hennacy and Jonikas 2020).

Cyanidioschyzon merolae is a photosynthetic aquatic organism which overcomes substantial barriers to inorganic carbon (Ci) acquisition and fixation. The common laboratory strain of this extremophilic red microalga, *C. merolae* 10D, was first isolated from the Italian volcanic caldera Campi Flegrei and is optimally cultured at pH 1.5–2.5 and temperature 42–45 °C (De Luca et al. 1978; Albertano et al. 2000; Miyagishima and Wei 2017). Ci concentrations in *C. merolae*'s natural environment likely span a significant range, as Campi Flegrei's carbon output varies over time,

✉ Berkley J. Walker
berkley@msu.edu

[1] Department of Plant Biology, Michigan State University, East Lansing, MI, USA

[2] Michigan State University - Department of Energy Plant Research Laboratory, Michigan State University, East Lansing, MI, USA

and the waters of this volcanic system vary considerably in Ci content (Venturi et al. 2017; Chiodini et al. 2021). In the laboratory, ambient concentrations of CO_2 are sufficient for cultivation of *C. merolae*. Supplying 5% CO_2 in combination with increased light intensity accelerates *C. merolae*'s growth, but under constant light this alga maintains similar growth rates when transitioned between 0.04% and 5% CO_2 (Minoda et al. 2004; Rademacher et al. 2016; Miyagishima and Wei 2017). High-temperature and low-pH conditions limit CO_2 solubility and restrict the accumulation of dissolved Ci species other than CO_2, which readily outgasses from aqueous environments (Oesterhelt et al. 2007). The resulting Ci scarcity likely presents an obstacle to growth of *C. merolae*, as this alga appears to depend on phototrophy. The only known method for heterotrophic culture of wild-type *C. merolae* requires supplying cells with glycerol concentrations far higher than are typical in natural or laboratory conditions, and the resulting heterotrophic growth is slow and ceases after 6–7 cell divisions (Moriyama et al. 2015, 2017, 2018; Liu et al. 2020). Accordingly, genomic data suggests that *C. merolae* may have a relatively limited capacity for organic carbon uptake: *C. merolae*'s genome has substantially fewer putative carbohydrate transporters and glycerol permeases than the genome of a closely related facultative heterotroph (Weber et al. 2004; Barbier et al. 2005; Fujiwara et al. 2019). How *C. merolae*'s photosynthesis is adapted to its extreme environment, including whether the organism has a CCM, is not well-understood. Most biophysical CCMs involve uptake of the Ci species bicarbonate, which is more easily concentrated within membranes than CO_2 (Mangan et al. 2016). However, bicarbonate is minimally available at low pH, presenting further challenges to Ci acquisition in *C. merolae*.

In addition to being an interesting system for the study of photosynthesis under extreme conditions, *C. merolae* is experimentally tractable due to its simple cellular and metabolic structures, its highly reduced and completely sequenced genome, and its amenability to molecular techniques (Matsuzaki et al. 2004; Kuroiwa et al. 2017). Further studies of *C. merolae* will expand our knowledge of the phylogenetically remote algae order Cyanidiales, which includes the only eukaryotes and phototrophs known to tolerate the conditions of acidic sulfur-rich geothermal springs (Miyagishima et al. 2017; Stadnichuk and Tropin 2022). This unique environmental resilience suggests that Cyanidiales hold promise for production of biofuels and other high-value algal products. For example, Cyanidialean algae like *C. merolae* and *Galdieria* species are of biotechnological interest in part because they can grow in wastewater and in environments which inhibit the growth of the culture-contaminating organisms that commonly plague aquaculture (Varshney et al. 2015; Sato et al. 2017; Lang et al. 2020; di Cicco et al. 2021). Understanding mechanisms by which Cyanidiales increase carbon capture efficiency may thus have biotechnological value.

CCMs by definition substantially accumulate intracellular inorganic carbon, as is detectable in *C. merolae* (Zenvirth et al. 1985). However, the existence of the CCM in *C. merolae* is uncertain due to the necessity of a functional photorespiratory pathway in this alga and to variation in this alga's CO_2 compensation point with O_2 concentration (Rademacher et al. 2016; Parys et al. 2021). Here we show that *C. merolae* exhibited CO_2 uptake characteristics that are unlikely to be explained by rubisco's kinetic properties alone. In particular, we show that *C. merolae* exhibited the gas-exchange features which are outcomes of all CCMs: low CO_2 compensation point, high affinity for external CO_2, and minimized rubisco oxygenation. The carbon isotope composition of *C. merolae*'s biomass was also consistent with a CCM. Additionally, our gas-exchange measurements indicated that *C. merolae* primarily takes up Ci as CO_2, rather than bicarbonate. We use homology to known CCM components to propose a model of a unique pH-gradient-based CCM, and we discuss how this model may be investigated in *C. merolae*.

Results

Cyanidioschyzon merolae's CO2 compensation point, affinity for CO2, and oxygen response are not fully explained by rubisco kinetics of thermophilic red algae

To determine whether *C. merolae* shows gas-exchange features consistent with the operation of a CCM, we measured the cellular CO_2 compensation point (Γ_{CO_2}) and affinity for CO_2 ($K_{m(CO_2)}$) under varying temperature and oxygen conditions. CCMs can boost photosynthetic efficiency beyond what is explainable by an organism's rubisco kinetics (Raven and Beardall 2003; Giordano et al. 2005). Therefore, we built a quantitative framework for interpreting our gas exchange data by calculating the Γ_{CO_2} and $K_{m(CO_2)}$ permitted by combinations of the rubisco kinetic parameters of thermophilic red algae, assuming the absence of a CCM or of ribulose 1,5-bisphosphate (RuBP) limitation. Details on these calculations are provided in the Methods section, and Table 1 lists the inputs used for calculations (including values from Fig. S1), parameter definitions, and input values.

Measured Γ_{CO_2} values were lower than the calculated ranges, meaning that net carbon assimilation was able to occur at lower CO_2 concentrations than would be expected in the absence of a CCM. Additionally, rubisco CO_2 affinity (K_c) values (once adjusted for temperature) could be compared to a measured cellular $K_{m(CO_2)}$, since *C. merolae*'s carbon assimilation showed a Michaelis–Menten-like response to CO_2 availability (Fig.

Table 1 Parameters used in model calculations of gas-exchange parameters from rubisco kinetics

Parameter	Definition	Value(s)	Source(s)
$S_{c/o}$	The CO_2/O_2 specificity of rubisco (ratio of the carboxylase to oxygenase rate when CO_2 and O_2 are present at equal concentrations), here presented in molar/molar (liquid-phase) form	224.6 (*Cyanidium caldarium)* 238.1 (*Galdieria partita)* 166 (*Galdieria sulphuraria)*	Uemura et al. (1997); Whitney et al. (2001)
K_c	The Michaelis–Menten constant of rubisco for CO_2	6.7 µM (*Cyanidium caldarium)* 6.6 µM (*Galdieria partita)* 3.3 µM (*Galdieria sulphuraria*)	Uemura et al. (1997); Whitney et al. (2001)
K_o	The Michaelis–Menten constant of rubisco for O_2	374 µM (*Galdieria sulphuraria*)	Whitney et al. (2001)
R_L / V_{cmax}	The ratio of CO_2 loss in the light, R_L, to rubisco's maximal rate of carboxylation, V_{cmax}	0.13 (40 °C) 0.07 (30 °C)	This study; ratio of cellular R_L to cellular maximal assimilation rate, A_{max}, as determined from light response curve (Fig. S1)
O	Chloroplastic O_2 concentration	20 µM (2% O_2 atmosphere, 40 °C) 209 µM (21% O_2 atmosphere, 40 °C) 398 µM (40% O_2 atmosphere, 40 °C) 251 µM (21% O_2 atmosphere, 30 °C)	This study; Henry's Law estimates
$H_{298.15}$	Standard-temperature Henry's law constant	0.035 mol/(kg*bar) (CO_2) 0.0012 mol/(kg*bar) (O_2)	NIST
$\frac{-\Delta_{sol}H}{R}$	Temperature dependence constant used to adjust standard-temperature Henry's law constants	2400 K (CO_2) 1700 K (O_2)	NIST
Q_{10}	Temperature coefficient used to calculate how a parameter's value would respond to 10 °C temperature shifts	0.60 (Q_{10} (25 °C) for $S_{c/o}$ values in the liquid phase) 0.62 (Q_{10} (35 °C) for $S_{c/o}$ values in the liquid phase) 2.24 (Q_{10} (25 °C) for K_c values in µbar) 1.63 (Q_{10} (25 °C) for K_o values in mbar)	von Caemmerer (2000); Galmés et al. (2016)

S2). Measured cellular $K_{m(CO_2)}$ values overlapped only with the temperature-corrected K_c values from *Galdieria sulphuraria* rubisco, which are the lower bounds of the calculated rubisco $K_{m(CO_2)}$ ranges (Fig. 1). Literature values of $K_{m(CO_2)}$ and Γ_{CO_2} had varying degrees of overlap with our calculated values (Fig. 1).

CCMs minimize rubisco oxygenation and thus reduce the response of characteristics of CO_2 assimilation to oxygen. For example, in the extreme case of an organism with a CCM that completely inhibits rubisco's oxygenase activity, there would be no oxygen sensitivity of CO_2 assimilation parameters affected by rubisco oxygenation (such as Γ_{CO_2}). In the case of an organism with an imperfect but functional CCM, the oxygen response of Γ_{CO_2} would be reduced compared to the oxygen response calculated from rubisco kinetics, and this is what appears to have occurred in *C. merolae*. Across all tested oxygen concentrations (2%, 21%, 40%), Γ_{CO_2} had a lower value than that calculated from rubisco kinetics, and additionally Γ_{CO_2} had a shallower oxygen-response slope than calculated from the rubisco kinetics. The measured slope was 5425 ± 1396 pM CO_2/µM O_2 (mean ± 2 SEs, $n = 6$) while the slopes calculated from rubisco kinetics were 7046–11,153 pM CO_2/µM O_2.

While these comparisons between measured and calculated Γ_{CO_2}, $K_{m(CO_2)}$, and oxygen response of Γ_{CO_2} were consistent with the presence of a CCM, the Γ_{CO_2} values and oxygen-response slope of Γ_{CO_2} were larger than those estimated for *C. reinhardtii* under comparable conditions (Fig. 2). The oxygen-response slope of Γ_{CO_2} calculated *C. reinhardtii* data was 2 pM CO_2/µM O_2.

The stable carbon isotope signature of *C. merolae*'s biomass is isotopically heavier than that of some photosynthetic organisms lacking CCMs

To further investigate whether *C. merolae* shows signatures of a CCM, we determined its biomass $\delta^{13}C$. *C. merolae*'s biomass $\delta^{13}C$ is heavier than is typical for multiple classes of organisms without CCMs (many C_3 plants, as well as macroalgae and seagrasses that likely do not uptake bicarbonate) (Table 2). However, it is isotopically lighter than literature values for organisms with

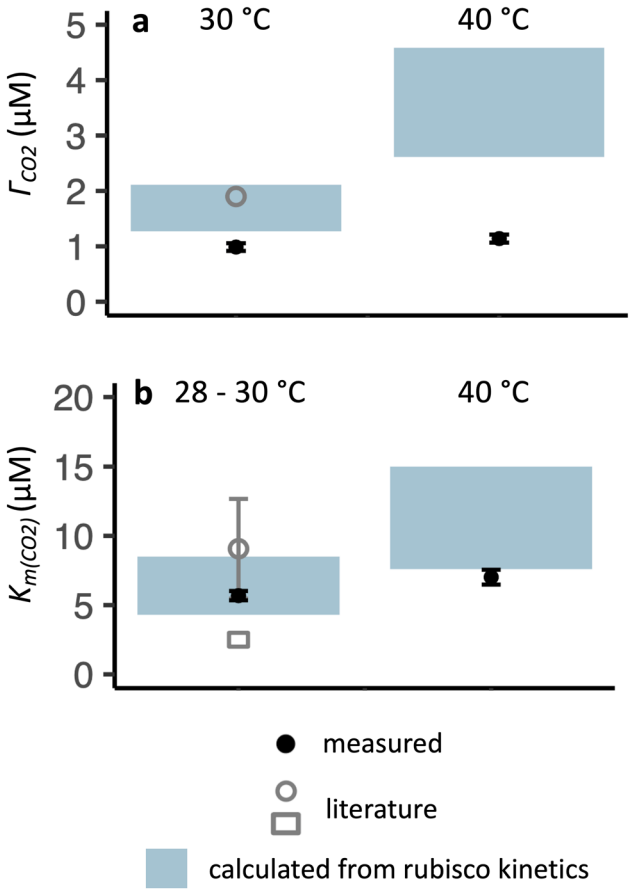

Fig. 1 Comparison of gas exchange parameters calculated from rubisco kinetics of thermophilic red algae (shaded areas) to measured gas exchange parameters (black solid points, means of $n=3$ replicates, with error bars indicating ±2 SEs), and to literature values (gray open shapes, presented as ranges or as mean ±2 SEs when available). The parameters examined are **a** Γ_{CO_2} and **b** $K_{m(CO_2)}$. In **b**, the measured and literature values represent the cellular $K_{m(CO_2)}$, while the calculated values represent the rubisco K_c. The literature data sources are Zenvirth et al. (1985); Rademacher et al. (2016); Parys et al. (2021), which report oxygen evolution data across external pH 1.5–7.5, oxygen evolution data from cells grown under 5% CO_2 and exposed to ambient CO_2 concentrations for 24 h, and a compensation point measurement at 21% O_2, respectively

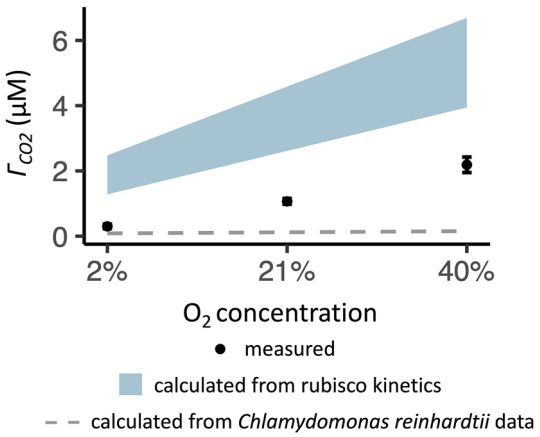

Fig. 2 Oxygen response of Γ_{CO_2} in *C. merolae*. The measured Γ_{CO_2} (points mean ±2 SEs, 6 total samples in a gas-exchange system supplied with 21% O_2 and 2% or 40% O_2) is compared to compensation points calculated from the rubisco kinetics of thermophilic red algae (shaded areas) or from published data on oxygen and temperature response of *C. reinhardtii* (dashed lines). *C. reinhardtii* data is from Coleman and Colman (1980)

CCMs (C_4 plants, CCM-containing microalgae, and macroalgae and seagrasses that likely uptake bicarbonate) (Table 2).

Cyanidioschyzon merolae predominantly takes up CO_2, rather than bicarbonate

To reveal which Ci species is taken up by *C. merolae*, we conducted gas-exchange measurements in cells resuspended at pH 2 or pH 6 (Fig. 3), since pH affects Ci speciation. Bicarbonate is minimally available at pH 2 but comprises approximately half of the Ci pool at pH 6, while aqueous CO_2 is expected to be similarly available between the two pH conditions. Therefore, if *C. merolae* could take up bicarbonate in addition to CO_2, its accessible Ci pool would be about twice as large at pH 6 than for pH 2 under the same headspace CO_2 concentration (Fig. 4). Although there was a decrease with increased pH in $K_{m(CO_2)}$ and, perhaps relatedly, a decrease in A_{max}, the decrease in $K_{m(CO_2)}$ was not of the magnitude that would be expected if *C. merolae* takes up bicarbonate. Furthermore, there was no decrease in Γ_{CO_2} with increased pH ($\alpha=0.05$; $p>0.99$ for Γ_{CO_2} and $K_{m(CO_2)}$ from unpaired *t*-tests with the alternative hypotheses being that the pH 6 parameter means are half of the pH 2 parameter means; $p=0.04$ for $K_{m(CO_2)}$, 0.97 for Γ_{CO_2}, and 0.0003 for A_{max} from unpaired *t*-tests with the alternative hypothesis being that the pH 2 parameter means are greater than pH 6 parameter mean). Overall, these gas-exchange results (Fig. 3) indicated that *C. merolae* primarily takes up Ci as CO_2, even when bicarbonate is available.

Cyanidioschyzon merolae has homologs to known CCM components

To generate ideas about how the CCM might operate in *C. merolae*, we identified a number of putative homologs to CCM components in *C. merolae*'s genome (Table S1). Notably, we identified two candidates for carbonic anhydrases potentially involved in the CCM (CMI270C, CMT416C) and six candidates for bicarbonate transporters potentially involved in the CCM (CMO283, CMK129C, CMN251C, CMI052C, CMR009C, CMN088C) (Table 3). Some of these candidates have a transcriptional response to CO_2 (Rademacher et al. 2017) and/or are reciprocal best hits with their query CCM gene, which is consistent with their having a role in the CCM. CCM components with no apparent homologs in *C. merolae* appear to include components

Table 2 Biomass $\delta^{13}C$ in *C. merolae* (mean ± 2 SEs, $n = 4$) and benchmark $\delta^{13}C$ values

Sample type	$^{\delta 13}C$	Source
Dssolved bicarbonate	~0‰	Raven et al. (2002)
Ambient air in laboratory building, evening	−9.56‰	This study
Marine macroalgae and seagrasses which are likely to uptake bicarbonate	> −10‰	Raven et al. (2002)
C_4 plants	−12 to −16‰ (usually approximately -14‰)	O'Leary (1988)
Various CCM-containing microalgae	−15 to −21‰ (*C. reinhardtii*: −18 or −19‰)	Wu et al. (2012); Goudet et al. (2020)
C. merolae	−23.03 ± 0.16‰	This study
C_3 plants	−20 to −37‰ (estimated global average: −28.5‰)	Kohn (2010)
Marine macroalgae and seagrasses which are unlikely to uptake bicarbonate	< −30‰	Raven et al. (2002)

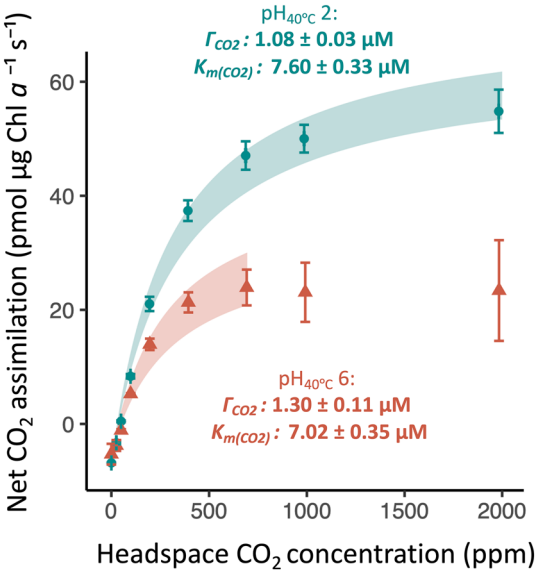

Fig. 3 CO_2 response of cells grown at pH 2.7 and assayed at pH 2 (blue fit and points) or 6 (red fit and triangles) (points and error bars represent mean ± 2 SEs, $n = 3$). A two-parameter Michaelis–Menten curve was fit to all points (pH 2) or to points < 700 ppm (pH 6), and the shaded areas indicate the range of values produced by combining the upper and lower bounds of the calculated Michaelis–Menten parameters (bounds of a 95% confidence interval)

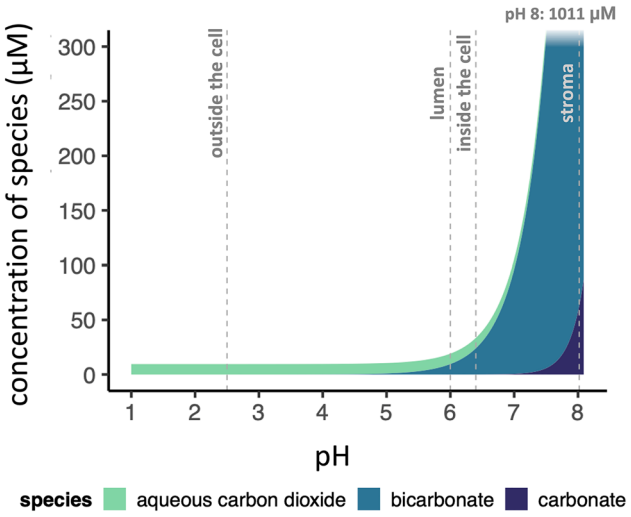

Fig. 4 Calculated Ci concentrations in pure water (conditions: 40 °C, 1013.25 hPa, water surface at 400 ppm CO_2, aqueous CO_2 concentrations constant across pH). pH benchmarks of interest are indicated, including potential pH conditions outside the cell (the optimal growth pH of *C. merolae*), in the thylakoid lumen (the approximate thylakoid lumen pH of unstressed plants in the light), inside the cell (the average intracellular pH of *C. merolae*), and in the stroma (the stromal pH of spinach chloroplasts in the light). This image is not intended to precisely represent Ci concentrations inside the cell (which could be affected by a number of factors, including various disequilibriums and the presence of other solutes). The y-axis is truncated at 300 µM to provide better visibility of trends at acidic pH. Sources for pH benchmarks: Werdan et al. (1975); Zenvirth et al. (1985); Kramer et al. (1999); Miyagishima and Wei (2017)

that are inessential to or indirectly involved in the algal CCM (e.g., some pyrenoid components, transcriptional regulators, proteins involved in energization of Ci uptake, and additional carbonic anhydrases and Ci transporters) (Table S1).

Discussion

Gas-exchange and carbon isotope evidence for a CCM in *C. merolae*

C. merolae's Γ_{CO_2} and $K_{m(CO_2)}$ are consistent with a functioning CCM. *C. merolae* maintained a lower Γ_{CO_2} (Fig. 1) and shallower oxygen response of Γ_{CO_2} (Fig. 2) than would be expected without a CCM, as evidenced by comparisons to Γ_{CO_2} values calculated using the rubisco kinetics from other thermophilic red algae. Furthermore, *C. merolae*'s cellular $K_{m(CO_2)}$ is low enough that it overlaps only with the temperature-corrected rubisco K_c measured in *G. sulphuraria* (Fig. 1), which is the lowest-known K_c (Flamholz

Table 3 Select *C. merolae* loci identified as homologs to CCM-involved genes in other organisms

Gene in *C. merolae* and its annotation	Homologous CCM-involved gene	Percent identity / E score	Predicted localization in *C. merolae*	Transcript abundance response to shift from high to ambient CO_2 (Rademacher et al. 2017)	Reciprocal best hit
Carbonic anhydrases					
CMI270C, "similar to carbonic anhydrase precursor"	*ecaA*, an α-class carbonic anhydrase of *Synechococcus elongatus* strain PCC 7942	46% / 3e-8	Other, other	0.5-fold at 24 h	Yes
	CAH1, CAH2, and *CAH3*, α-type periplasmic or lumenal carbonic anhydrases of *C. reinhardtii*	44 – 46% / 5e-5 – 6e-6			Yes (*CAH3*)
CMT416C, "similar to carbonic anhydrase precursor"	same as above	45% / 2e-7	Thylakoid lumen, chloroplast	65-fold at 3 h, 32-fold at 24 h	Yes
		33–39% / 4e-5–8e-4			Yes (*CAH3*)
Bicarbonate transporters					
CMO283, "unknown ABC anion transporter"	*cmpB,* a gene in the operon encoding the ATP-dependent bicarbonate transporter BCT1 of *Synechocystis PCC6803*	24% / 8e-5	Thylakoid lumen, other	Not significant	Yes
CMK129C, "nitrate ABC transporter ATP-binding protein"	*cmpC* and *cmpD*, genes in the operon encoding the ATP-dependent bicarbonate transporter BCT1 of *Synechocystis* PCC6803	41% / 6e-39 and 3e-43	Thylakoid lumen, chloroplast	Not significant	No
CMN251C, "ATP-binding cassette, sub-family C (MRP), member 1"	*HLA3,* an ATP-binding cassette transporting Ci at the plasma membrane of *C. reinhardtii*	40% / 1e-112	Other, chloroplast	1.9-fold at 3 h	No
CMI052C, "probable sulfate permease"	*bicA,* a sodium-dependent sulfate-permease-type bicarbonate transporter of *Synechocystis* PCC6803	21% / 1e-28	Thylakoid lumen, chloroplast	2.2-fold at 24 h	No
CMR009C, "probable anion transporter"	*PtSLC4-2* and four other *PtSLC4* genes, which are putative sodium-dependent transporters of extracellular bicarbonate of *Phaeodactylum tricornutum*	26 to 48% / 8e-52 to 1e-132	Other	1.6-fold at 24 h	Yes (*PtSLC4-6*)
CMN088C, "hypothetical protein, conserved"	*BST1,* a candidate for a thylakoid bicarbonate transporter of *C. reinhardtii*	26% / 8e-3	Other, secretory pathway	Not significant	No

Localization predictions (TargetP, PredAlgo) of "other" may include targeting to the cytosol, while predictions of "secretory pathway" may include targeting to the endoplasmic reticulum or cytoplasmic membrane (Mori et al. 2016). Otherwise, these tools do not indicate whether proteins may be transported into a membrane. Transcript abundance analysis is sourced from Rademacher et al. (2017), and "significant" transcript responses are those with Bonferroni-corrected q-value < 0.01 for comparisons between the high-CO_2 timepoint and an ambient-CO_2 timepoint (3 or 24 h after shift to ambient CO_2). All *C. merolae* genes are top hits of their respective queries, except for CMT416C, which was the second hit of its listed queries. For full homology results and sources for CCM-involved genes, see Table S1

et al. 2019). A $K_{m(CO_2)}$ lower than K_c most likely arises from a CCM (Raven et al. 2011).

The biomass $\delta^{13}C$ of *C. merolae* is also consistent with a CCM, though numerous environmental and physiological factors impact carbon isotope fractionation in biological material (Sharkey and Berry 1985; O'Leary 1988; Raven and Beardall 2003; Hurley et al. 2021). For example, the extracellular δ^{13} Ci signature varies according to growth environment, and the amount of ^{13}C available to *C. merolae* cells would be limited by the low-bicarbonate aqueous growth conditions of this alga. Dissolved bicarbonate has an isotopically heavier $\delta^{13}C$ than CO_2 (Table 2), and the slower diffusion of isotopically heavier dissolved Ci species (Raven et al. 2002) may be less significant for bicarbonate than for CO_2, which has a lower molecular weight. Additionally, stable carbon isotopes show an increased solubility of isotopically lighter molecules compared to isotopically heavier molecules, and this effect reduces only very slightly with temperature (Vogel et al. 1970). Despite these constraints on ^{13}C availability in *C. merolae*'s growth environment, *C. merolae* had a heavier $\delta^{13}C$ signature than many photosynthetic organisms which lack a CCM (Table 2). This suggests that *C. merolae*'s biomass $\delta^{13}C$ is compatible with a stromal environment that limits rubisco's discrimination against $^{13}CO_2$, i.e., the environment produced by a CCM. Interestingly, *C. merolae* had a lighter $\delta^{13}C$ signature than *C. reinhardtii*, which could result from a more efficient CCM in *C. reinhardtii* (Table 2). *C. merolae*'s CCM form is not sufficiently resolved to determine its CCM efficiency via Ci accumulation ratios; for example, to resolve *C. merolae*'s Ci accumulation ratios with ^{14}Ci centrifugation-filtration, it will be necessary to improve understanding of pH and Ci compartmentalization in this alga (Zenvirth et al. 1985). However, the proposition of a CCM in a possibly pyrenoidless alga (Broadwater and Scott 1994; Badger et al. 1998; Albertano et al. 2000; Misumi et al. 2005) which relies on CO_2 uptake (Fig. 3) is consistent with relatively low Ci accumulation. *C. reinhardtii* cells accumulate Ci up to 40-fold and achieve internal Ci concentrations 5-to-tenfold higher than mutants and morphologically similar species without pyrenoids (Badger et al. 1980; Morita et al. 1998; Meyer et al. 2017). CCMs relying on CO_2 uptake alone may accomplish only 10-to-15 fold Ci accumulation (Gross 2000). The modest efficiency of *C. merolae*'s CCM is also suggested by the higher Γ_{CO_2} and stronger oxygen response of Γ_{CO_2} in *C. merolae* as compared to the response of *C. reinhardtii* estimated under comparable conditions (Fig. 2). It will be interesting to further investigate the factors that shaped the evolution of this modest CCM.

C. merolae's rubisco kinetics, though unknown, are unlikely to explain our gas-exchange observations. *C. merolae*'s gas-exchange physiology was not fully explained by the rubisco kinetics of other thermophilic red algae (Figs. 1, 2), which include the highest known rubisco $S_{c/o}$ and lowest known K_c. Rubisco kinetics are highly constrained (Flamholz et al. 2019), so it seems improbable that *C. merolae*'s rubisco specificity and affinity would be so high as to explain this alga's Γ_{CO_2} physiology. When we added to our model a temperature-adjusted $S_{c/o}$ of double the highest temperature-adjusted value and a K_c of half the lowest temperature-adjusted value, we calculated a Γ_{CO_2} of 1.3, still slightly higher than *C. merolae*'s Γ_{CO_2} of 1.1 µM at low pH, 40 °C, and 21% O_2 (Fig. 1, Fig. 3). Furthermore, the existence of the CCM in *C. merolae* is supported by direct evidence of intracellular Ci concentration in *C. merolae* (Zenvirth et al. 1985).

Characterization of *C. merolae*'s rubisco will further reveal the drivers of carbon capture efficiency in this alga. *C. merolae*'s rubisco belongs to the subform ID lineage, which is currently associated with high specificity and affinity for CO_2, especially in organisms without pyrenoids. However, the subform ID lineage has not been extensively characterized (Badger et al. 1998; Giordano et al. 2005; Loganathan and Tsai 2016; Iñiguez et al. 2020), and CCMs may have various evolutionary relationships with rubisco kinetics. For example, CCMs may relax pressure for an organism to improve rubisco's CO_2 affinity and specificity (Young et al. 2012; Iñiguez et al. 2020); if such a relaxation occurred in *C. merolae*, it would be all the more indicative of a CCM that *C. merolae*'s cellular $K_{m(CO_2)}$ is lower than all known temperature-adjusted rubisco K_c values save one (Fig. 1b).

A potential pH-gradient-based CCM in *C. merolae* invites further characterization

Overview of potential CCM structure in *C. merolae*

Although it appears uncommon for microalgae to lack a CCM (Raven et al. 2011), and knowledge of what is typical for the CCM is still expanding, the apparent presence of a CCM in *C. merolae* is notable because it suggests the presence of a unique mechanism for carbon concentration. *C. merolae* maintained an apparent CCM in a low-bicarbonate external environment, which suggests the presence of a pH-gradient-based concentration of carbon relative to acidic surroundings. Dissolved CO_2, rather than bicarbonate, appeared to be the primary Ci species taken up by cells (Fig. 3). *C. merolae*'s reliance on CO_2 is also indicated by the variance of $K_{m(Ci)}$ of oxygen evolution with pH, and by ^{14}Ci pulse-chase experiments (Zenvirth et al. 1985). *C. merolae*'s reduced A_{max} at pH 6 or 5.5 compared to pH 2 or 1.5 (Fig. 3, Zenvirth et al. 1985) indicates that pH stress may impair function of acidophiles in near-neutral conditions. However, it seems reasonable that cells adapted and acclimated to low pH would not maintain bicarbonate uptake machinery, as taking up bicarbonate against a large bicarbonate gradient

may be prohibitively energetically expensive. Such a bicarbonate gradient (Fig. 4) may also support the CCM. pH-gradient-based CCMs have attracted interest as a possible CCM of acidophilic organisms (Gehl and Colman 1985; Weber et al. 2007; Rademacher et al. 2016). In this type of CCM, the maintenance of near-equilibrium Ci concentrations in a near-neutral cytosol would concentrate carbon relative to acidic surroundings, even if Ci enters the cell only by CO_2 diffusion. Bicarbonate accumulated in this cytosolic bicarbonate trap could then be transported into the chloroplast. The basic stroma could function as a second bicarbonate trap, as is proposed for *C. reinhardtii* (Fei et al. 2022).

Cyanidioschyzon merolae's CCM may depend on active transport

pH-gradient-based CCMs may be called "passive CCMs," which refers to the primary mode of Ci entry into the cell, rather than a lack of protein or energy investment in the CCM. In fact, there are proteins which could facilitate the operation of a passive CCM and which have homologs in *C. merolae* (Table 3, Table S1). In our hypothetical model of *C. merolae*'s CCM (Fig. 5), active bicarbonate transporters at the chloroplast envelope and thylakoid membrane overcome the low membrane-permeability of bicarbonate (Mangan et al. 2016). There are several types of bicarbonate transporters which have homologs in *C. merolae* (Table 3), though this homology analysis is complicated by the fact that known bicarbonate transporters, like many CCM-involved genes, belong to widespread protein families whose members have diverse functions. In our analysis, it was common to obtain numerous hits for bicarbonate transporter queries, and reciprocal best hits analysis was subject to limitations of the NCBI database (e.g., inclusion of similar sequences from different experiments in combination with limited annotation of species and functions). In addition to bicarbonate transporters, a passive CCM would depend on maintenance of near-neutral pH in the cytosol, which in *C. merolae* requires a large investment in synthesizing and operating plasma membrane H^+-ATPases. These proton pumps, which were found in one analysis to have the highest transcript abundance of any gene in *C. merolae*'s genome (Misumi et al. 2017), may consume up to 1 ATP per proton extruded into a low-pH extracellular environment (Zenvirth et al. 1985).

Carbonic anhydrases in the CCM

Carbonic anhydrase (CA) enzymes, which catalyze interconversion of Ci species, had homologs in *C. merolae*. CAs have diverse functions and not all CAs are involved in photosynthesis or a CCM, but these enzymes are part of the CCM in well-studied systems (Morita et al. 1998; Jensen et al. 2020). When a membrane-permeable CA inhibitor

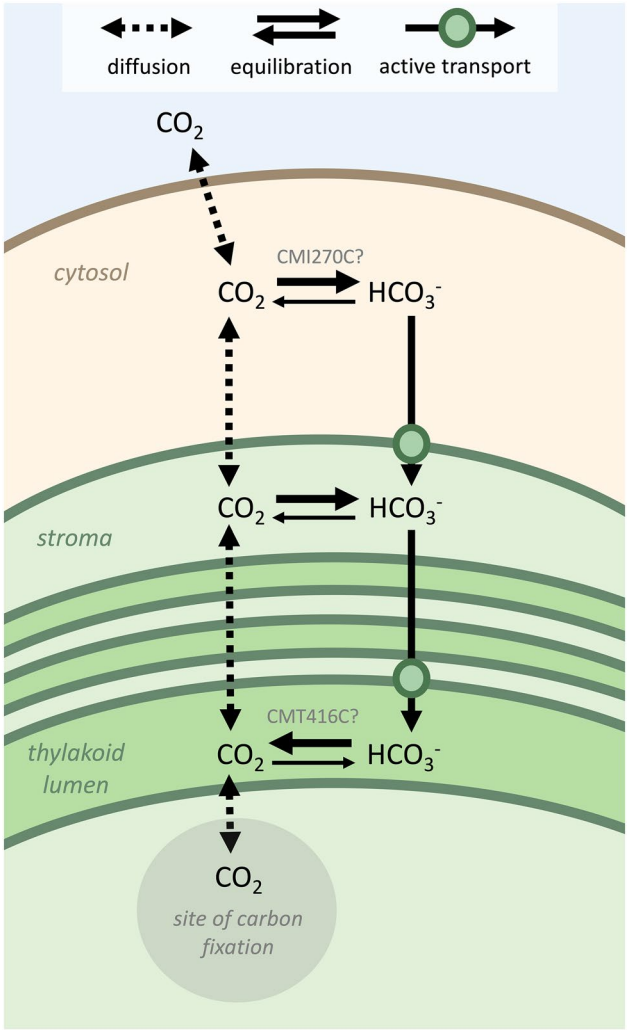

Fig. 5 Hypothetical model of the CCM in *C. merolae*, indicating how Ci species may diffuse, interconvert, and be transported to concentrate carbon around the site of rubisco carboxylation (more details in text). In pairs of equilibration arrows, the thicker arrow points to the Ci species which is predicted to be more abundant in that compartment (see Fig. 4) (arrows are not to scale with relative abundances of Ci species). This image abbreviates the movement of Ci through the outer thylakoid rings, which we hypothesize may occur by active transport across thylakoids or by diffusion through discontinuities in the thylakoids. Carbonic acid may represent a minor membrane-permeating species alongside CO_2

dissolved in DMSO was applied to *C. merolae* cells, cellular oxygen evolution did not decrease compared to DMSO alone (Moroney et al. 2004; Parys et al. 2021). However, the presence of CA homologs in *C. merolae*'s genome is consistent with the operation of a biophysical CCM. In particular, we identified two α-CA homologs which we hypothesize participate in the CCM (Table 2). These putative α-CAs are among the four *C. merolae* CA candidates which have homology to *Arabidopsis thaliana* CAs, and their localizations by fluorescence tagging and their transcriptional

responses to CO_2 availability have been previously discussed (Rademacher et al. 2017). The other two CA candidates previously discussed, CMM052C and CMD023C, (Rademacher et al. 2017) were identified by us as homologs to mitochondrial γ-CAs (Table S1), and since their localization predictions and annotations suggested mitochondrial functions, we did not include them in our model of the CCM.

CA localization and function invites further study in *C. merolae*, especially as the microalgal CCM is not as mechanistically well-understood as the cyanobacterial CCM, and molecular studies of microalgae other than *C. reinhardtii* are particularly sparse (Meyer and Griffiths 2013). It will be particularly useful to confirm where CAs function in the cell, as CCM function depends on proper CA localization. For example, the cyanobacterial CCM requires above-equilibrium bicarbonate concentrations in the cytosol and therefore depends on the absence of cytosolic CAs, while modeling of *C. reinhardtii*'s CCM suggests that CA distribution within an organelle would impact CCM function (Price and Badger 1989; Price et al. 2008; Fei et al. 2022). In *C. merolae*, a cytosolic CA, perhaps CMI270C (Rademacher et al. 2017), may be involved in cytosolic bicarbonate trapping. Another CA, perhaps CMT416C, may facilitate recapture of CO_2 released during mitochondrial glycine decarboxylation of photorespiration. This role of CMT416C is supported by CMT416C's predicted mitochondrial targeting sequence; by CMT416C's fluorescence-tag localization between *C. merolae*'s mitochondrion and chloroplast; and by the existence of C_2 photosynthesis, a plant carbon-concentrating mechanism which recaptures carbon from mitochondrial glycine decarboxylation (Sage et al. 2011; Rademacher et al. 2017). However, our model (Fig. 5) depicts an alternative function of CMT416C. CMT416C was predicted to have a chloroplast or thylakoid targeting sequence (Table 3) and thus we propose that CMT416C may be a thylakoid lumen enzyme with plastid import disrupted by fluorescence tagging. A thylakoid lumen CA, like CAH3 of *C. reinhardtii* (Moroney et al. 2011), may drive CO_2 release around rubisco after Ci is pumped to above-equilibrium concentrations in the stroma. Although we used localization prediction tools trained on organisms evolutionarily distant from *C. merolae*, these tools' plastidial localization predictions are often experimentally substantiated in *C. merolae*. For example, in *C. merolae*, plastidial localization predictions of acyl lipid metabolic enzymes from TargetP and PredAlgo are substantiated by fluorescence tagging in 72% (13/18) and 52% (14/27) of instances, respectively (Mori et al. 2016). TargetP plastidial localization predictions of *C. merolae*'s central carbohydrate metabolic enzymes are substantiated by fluorescence tagging in 89% (17/19) of instances (Moriyama et al. 2014). Tagging studies which engineer small additions onto carbonic anhydrases (i.e., epitope tag studies) or studies of functional complementation with fluorescence-tagged carbonic anhydrases would be useful to confirm these enzymes' location of function.

Proposition of a biophysical CCM in *C. merolae*

We did not include C_4 components in our CCM model, although the abundances of some C_4 pathway components respond to carbon availability in *C. merolae* and *G. sulphuraria* (Rademacher et al. 2017; Curien et al. 2021). In *C. merolae*, transcripts of the C_4 enzymes phosphoenolpyruvate carboxykinase (PEPCK), phosphoenolpyruvate carboxylase, and pyruvate phosphate dikinase increase in abundance following a shift from 5% CO_2 to 0.04% CO_2 conditions. Indeed, CCM components are often among those gene products upregulated by a shift to limiting CO_2, and the evolution of C_4 pathways may be relatively accessible and flexible, given the broad phylogenetic distribution of the necessary genes and the multiple evolutions of this pathway in plants (Hopkinson et al. 2016; Rademacher et al. 2017). However, the broad phylogenetic distribution of C_4 genes also means that many organisms have C_4 pathway components without a C_4 CCM, and it is unclear whether single-cell C_4 CCMs occur outside plants and macroalgae (von Caemmerer et al. 2014; Hopkinson et al. 2016; Jensen et al. 2020). *C. merolae*'s simple cellular structure may not permit an organizational structure analogous to the organelle partitioning that single-cell C_4 CCMs use to fulfill the spatial regulation requirements of C_4 photosynthesis (Edwards et al. 2004; Imoto and Yoshida 2017). Furthermore, a diffuse cytosolic localization of PEPCK in *C. merolae* (Moriyama et al. 2014) suggests that PEPCK decarboxylation is not directly involved in carbon concentration in this alga.

Chloroplast anatomy and the CCM

Unknown chloroplastic structural elements may also contribute to the CCM in *C. merolae*. Ultrastructural studies have not identified a recognizable pyrenoid in *C. merolae*, and this alga is described as lacking a pyrenoid (Broadwater and Scott 1994; Badger et al. 1998; Albertano et al. 2000; Misumi et al. 2005). Pyrenoids are membraneless organelles that support CCM function by aggregating rubisco into an environment conducive to efficient CO_2 fixation, and the presence of a pyrenoid is highly correlated with the presence of a CCM in algae; very few algal species are known to maintain a CCM in the absence of a pyrenoid (Badger et al. 1998; Morita et al. 1998; Meyer and Griffiths 2013; Hennacy and Jonikas 2020; Barrett et al. 2021). We note that *C. merolae*'s lack of chloroplastic carbohydrate structures is not inconsistent with the presence of a pyrenoid. Like other organisms with red plastids (plastids which are in red algae or were acquired by endosymbiosis of red algae) *C. merolae* stores starch in the cytosol (Takusagawa et al.

2016; Toyoshima et al. 2016). Presumably as a result of this cytosolic starch storage, pyrenoids in red plastids apparently never have starch sheaths, except in cases where the pyrenoid is located in a chloroplast protrusion (Barrett et al. 2021). It is also not particularly informative that there was no identified *C. merolae* homolog to the *C. reinhardtii* rubisco linker that facilitates pyrenoid formation (Table S1). Proteins mediating the formation of membraneless organelles often have stretches of low-complexity sequences that may complicate homology analysis (Wunder et al. 2019; Barrett et al. 2021). *C. merolae* did have homologs to *C. reinhardtii* pyrenoid components (*C. reinhardtii* methyltransferases, a PSII subunit, a protein localized to mesh-like structures between pyrenoid starch plates, and enzymes of starch synthesis), though these components could have pyrenoid-unrelated functions in *C. merolae* (Table S1). Thus, localization of rubisco or carbon fixation will be necessary to resolve the local environment of *C. merolae*'s rubisco. Another chloroplast structure of interest is the thylakoids, as thylakoid membranes are candidates for diffusion barriers to CO_2 (Barrett et al. 2021; Fei et al. 2022). *C. merolae*'s thylakoid membranes, which are arranged in concentric spheres and host arrays of very large light-harvesting complexes (Ichinose and Iwane 2017; Imoto and Yoshida 2017), may be particularly well-positioned to support a CCM.

Gas-exchange results suggest the importance of further exploring photorespiration in CCM-containing organisms

In addition to an apparent lack of a pyrenoid, *C. merolae* has several other characteristics which may at first seem unusual for an organism with a CCM. Transitions to low-Ci environments are associated with increased cellular affinity for CO_2 in some algae, presumably due to Ci-responsive expression of CCMs, but *C. merolae* cultures grown under 5% CO_2 do not show a significantly lowered $K_{m(CO_2)}$ of oxygen evolution when exposed to 0.04% CO_2 conditions for 24 h (Spalding and Portis 1985; Badger et al. 1998; Giordano et al. 2005; Rademacher et al. 2016). However, *C. merolae* does have a transcriptional response to changes in CO_2 availability, which includes shifts in the abundance of potentially CCM-involved transcripts (Rademacher et al. 2017). Even for the best-characterized algal CCM, that of the model alga *C. reinhardtii*, it is unclear how directly CCM physiology is tied to CO_2 supply. CCM strength and molecular mechanisms in *C. reinhardtii* vary according to factors such as the intensity of CO_2 limitation, the cellular division time in relation to the timing of environmental changes, and the presence of the photorespiratory byproduct and redox metabolite hydrogen peroxide (Vance and Spalding 2005; Mitchell et al. 2014; Wang and Spalding 2014; Neofotis et al. 2021). Furthermore, *C. reinhardtii*'s CCM is regulated by and requires light (Badger et al. 1980; Villarejo et al. 1996; Im and Grossman 2002), which suggests that induction of CCM physiology may be impacted by culture density and other conditions that are not directly related to CO_2 availability. *C. merolae*, like the soil-dwelling alga *C. reinhardtii*, lives natively in a dynamic environment and may have a similarly versatile CCM.

Other arguments for the absence of the CCM in *C. merolae* focus on the apparent significance of photorespiration in this alga. However, the known photorespiratory characteristics of *C. merolae* are in fact compatible with a CCM. For example, one argument against a CCM in *C. merolae* is that its Γ_{CO_2} is reduced to near-zero in 1.5% O_2 conditions but is 60 ppm in 21% O_2 conditions (Parys et al. 2021). One of the outcomes of all CCMs is indeed a minimized rubisco oxygenation reaction, and a Γ_{CO_2} of 60 ppm at 21% O_2 is indeed similar to the ~ 50 ppm reported for C_3 plants at 20 °C (Tolbert et al. 1995; Giordano et al. 2005). However, *C. merolae*'s gas-phase Γ_{CO_2} may not be directly comparable to the gas-phase Γ_{CO_2} of plants characterized at moderate temperatures since this comparison does not account for the barriers to Ci acquisition and use in high-temperature aqueous environments. Our measurements and analysis indicated that *C. merolae*'s gas exchange physiology was quantitatively compatible with a CCM (Figs. 1, 2).

Another photorespiration-based argument against *C. merolae*'s CCM is that *C. merolae* knockouts of a photorespiratory glycolate oxidase have a high-Ci-requiring phenotype, which is attributed to high fluxes through the photorespiratory pathway. High photorespiratory fluxes in *C. merolae* would stand in contrast to the low photorespiratory fluxes traditionally associated with CCM-containing organisms (Rademacher et al. 2016). Additionally, glycolate oxidation by a glycolate oxidase, rather than by a glycolate dehydrogenase, is associated with an absent or inefficient CCM in cyanobacteria and some algae (Hagemann et al. 2016). However, the photorespiratory pathway is known to be essential in organism with CCMs, including C_4 plants; CCM-containing algae; and cyanobacteria, which apparently always have CCMs (Raven et al. 2008; Moroney et al. 2013; Hagemann et al. 2016). Thus, necessity of the photorespiratory pathway cannot be diagnostic of an absent CCM. In fact, high glycolate oxidase activity is required for survival of the C_4 plant maize in ambient air (Zelitch et al. 2008). *C. merolae*'s use of a photorespiratory glycolate oxidase could be explained by inefficiencies of the organism's CCM (Table 2, Fig. 2), or by unique evolutionary factors influencing the development of *C. merolae*'s plant-type photorespiratory pathway. *C. merolae* has homologs to the nine enzymes of the *A. thaliana* photorespiratory pathway and to *A. thaliana* catalase, which detoxifies hydrogen peroxide produced by the photorespiratory pathway (Rademacher et al. 2016). Though *C. merolae* does not have close homologs to the plastidic

dicarboxylate transporters which function in photorespiratory nitrogen recycling in plants, this may be explained by some flexibility in the localization of photorespiratory nitrogen metabolism across organisms, like the flexible localization observed for ammonium assimilation in seed plants (Barbier et al. 2005; Marino et al. 2022). Overall, rubisco oxygenation is present in all studied oxygenic photosynthetic organisms, and there are likely evolutionary barriers to eliminating this process (Moroney et al. 2013). Future studies may provide more clarity on the magnitude and role of photorespiratory processes in *C. merolae* and in other organisms which possess a CCM.

Conclusion

We have described traits of *C. merolae* which are consistent with the operation of a CCM in this alga. Several aspects of this apparent CCM remain to be explored, including the CCM's enzymatic and structural components and the role of photorespiration in this organism. Characterizing these features of *C. merolae* will further reveal how this extremophilic red alga survives in an environment which challenges photosynthesis.

Methods

Cell culture

A plate of *C. merolae* 10D cells was kindly provided by Dr. Peter Lammers (Arizona State University). Our cultures were started from liquid inocula at OD_{750} ~ 0.1 and were grown at 40 °C under 100 µmol m^{-2} s^{-1} continuous white light. Cells were grown as 50 mL cultures in 250 mL Erlenmeyer flasks, in media prepared according to a modified version of the Cyanidium Medium recipe from the Culture Collection of Algae at The University of Texas at Austin. This growth medium as prepared contained 3.78 mM $(NH_4)_2SO_4$, 0.057 mM K_2HPO_4, 0.041 mM $MgSO_4 \cdot 7H_20$, 0.0015 mM $CaCO_3$, and 1 mL solution per L media of Hutner's Trace Elements. The medium was adjusted to pH 2.7 at room temperature by the addition of HCl. Cultures were aerated by shaking (50 rpm).

Measurements of CO_2 flux

Cells were harvested by spinning down ~ 5 mL culture samples (OD_{750} 1.2–1.7, 6–9 µg Chl *a* mL^{-1}) at 300 × *g* for 10 min. Cells were then gently resuspended to 2 µg Chl *a* mL^{-1} (OD_{750} ~ 0.4, 15 mL samples) and loaded into the LI-6800 Aquatic Chamber (LI-COR Biosciences). The samples were resuspended in fresh growth medium prepared as described above, except for pH experiments, where samples were resuspended in growth medium with a pH of 2 at 40 °C, or in growth medium with a pH of 6 at 40 °C. To determine chlorophyll content for this resuspension, 1 mL cell samples were centrifuged (18,407 × *g*) for 5 min at room temperature. The cell pellet was then concentrated into 100 µL growth medium, and the concentrated cells were mixed by vortexing with 900 µL ice-cold methanol. After 30 min of dark incubation on ice, cell debris was pelleted out of the sample by centrifugation (18,407 × *g*) for 5 min at room temperature, and the absorbance of the resulting supernatant was analyzed on a Cary 60 UV–Vis spectrophotometer (Agilent Technologies). Like cyanobacteria, *C. merolae* does not have chlorophylls other than chlorophyll *a* (Cunningham et al. 2007). Thus, we used the spectrophotometric chlorophyll *a* concentration calculation equation published by Ritchie (2006) for cyanobacterial extracts in methanol, with a correction for extract turbidity at 720 nm.

The aquatic chamber temperature was maintained at 30 or 40 °C by use of a recirculating water bath and the instrument's heat block temperature control function. Unless otherwise noted, the reference CO_2 setpoint was 400 ppm, the light setpoint was 50% red 50% blue with 2000 µmol m^{-2} s^{-1} incident on the sample (~ 1100–1200 µmol m^{-2} s^{-1} absorbed by sample), and other environmental parameters were set as follows: flow of 400 µmol s^{-1}, reference H_2O control at least 20 mmol mol^{-1}, fan speed of 14,000 rpm, subsample pump speed as set by 4.5 V direct current. The wait time between environmental condition changes and data logging was at least 480 s. Wait times were sufficient for fluxes to stabilize at least 1–2 min before logging, and exceeded the time needed for the media to adjust to changing CO_2 concentrations (Fig. S3). The sample chamber was triple rinsed with deionized water between media or sample injections, and samples were examined under a light microscope after measurement to confirm the absence of contamination.

All parameters of interest were expressed in terms of headspace CO_2 concentrations. Headspace CO_2 concentrations were calculated using the concentration difference between the sample chamber CO_2 concentration and headspace CO_2 concentration (ΔC_{sub}), as described in the manufacturer's documentation: $\Delta C_{sub} = \frac{\mu_i}{\mu_{i_{sub}}} \Delta C$. ΔC_{sub} was calculated using the sample flow rate (μ_i), the subsample loop flow rate ($\mu_{i_{sub}}$, measured as 233 µmol s^{-1}), and the difference between the sample and reference chamber CO_2 concentrations (ΔC). To make the determination of headspace CO_2 concentration using ΔC_{sub}, we assumed that when reference chamber CO_2 concentrations are higher than sample CO_2 concentrations, sample chamber CO_2 concentrations are higher than headspace CO_2 concentrations. Negative

headspace CO_2 concentrations were replaced with zeroes before data analysis.

An averaging time of 19 s was used when logging data. Matching of the sample and reference analyzers was performed when the $\Delta CO_2 < 10$ ppm, if the reference chamber CO_2 changed by > 100 ppm, or if the time between matches was > 30 min. In practice, this typically resulted in matching for each measured point.

During experiments examining the effect of oxygen concentration, a gas mixing system was used to introduce v/v mixes of 60% nitrogen / 40% oxygen, 79% nitrogen / 21% oxygen, or 98% nitrogen / 2% oxygen into the instrument at 1.5 standard liters per minute. The instrument's CO_2 injection system was then used to control CO_2 abundance in the headspace. Samples were exposed to 21% oxygen conditions, then to 2% or 40% oxygen conditions, then again to 21% oxygen conditions to confirm that minimal shifting of photosynthetic fluxes had occurred during the experimental period.

Michaelis–Menten parameters ($K_{m(CO_2)}$, A_{max}) were determined by using the R package "drc" (Version 3.0–1; Ritz et al. (2015)) to fit a two-parameter Michaelis–Menten equation to each replicate. CO_2 compensation point was determined by fitting a linear trendline to CO_2 response points ≤ 100 ppm CO_2 in each replicate. Light respiration (R_L) values were obtained by the Kok method, using the extrapolated intercept of a linear fit to points in each replicate with 10–30 µmol m^{-2} s^{-1} incident on the sample (~ 5.5–16.7 µmol m^{-2} s^{-1} absorbed by sample).

Modeling gas-exchange parameters

Calculations were performed in R (R version 3.6.0). Parameter definitions, values, and sources not listed in the Methods are provided in Table 1.

CO_2-O_2 interactions in photosynthetic organisms and their impact on Γ_{CO_2} are mechanistically well-understood, permitting the calculation of the CO_2 compensation point Γ_{CO_2} from rubisco kinetics and other information (von Caemmerer 2000): $\Gamma_{CO_2} = \frac{(0.5/S_{c/o}+(K_cR_L)/(K_oV_{cmax}))}{(1 - R_L/V_{cmax})}O + \frac{K_c(R_L/V_{cmax})}{(1 - R_L/V_{cmax})}$. Additionally, K_c values are of interest for comparison to the cellular $K_{m(CO_2)}$.

The kinetics of *C. merolae*'s rubisco are not known; recent collections of rubisco kinetics do not list kinetics for *C. merolae*'s rubisco (Young et al. 2016; Cummins et al. 2018; Flamholz et al. 2019), and to our knowledge these kinetics are not available elsewhere in the literature. Therefore, our calculation of Γ_{CO_2} used all combinations of the reported rubisco kinetics of thermophilic Cyanidialean red algae closely related to *C. merolae* (see Miyagishima et al. (2017) for a rubisco-based phylogenetic tree of these organisms).

Reported rubisco kinetics were measured at 25 °C. However, we needed a quantitative framework to interpret gas-exchange parameters measured at 30 and 40 °C, as increasing temperatures challenge carboxylation by limiting rubisco's CO_2 affinity and specificity. We therefore adjusted each kinetic parameter to $T = 30$ or 40 °C as in von Caemmerer (2000): $Parameter(T) = Parameter(25°C)Q_{10}^{\left[\frac{T-25}{10}\right]}$. To convert between the gas and liquid phase during temperature adjustments and elsewhere (calculating dissolved oxygen concentrations, converting physiological parameters from headspace concentrations to dissolved concentrations), we assumed an equilibrium defined by Henry's law $C = HP$, where C is the concentration of a dissolved gas, H is the Henry's law constant, and P is the gas partial pressure, which we calculated at an air pressure of 101,325 Pascal. Henry's law constants vary with temperature, so the following equation was used to adjust the standard-temperature constants $H_{298.15}$ to be appropriate for temperature $T = 303.15$ or 313.15 K according to $H(T) = H_{298.15}\exp[\frac{-\Delta_{sol}H}{R}\left(\frac{1}{T} - \frac{1}{298.15}\right)]$. Henry's law constants also vary according to the presence of other solutes in the solution, but this small effect is extremely difficult to estimate due to partially non-additive effects of solutes, and it is typically ignored by the rubisco community (Galmés et al. 2016). Some unit conversions required knowing the density of water at different temperatures, which we determined using a second-order polynomial fit to the water density values from Fierro (2007).

The rubisco V_{cmax} was estimated using the measured A_{max} of cell samples (Table 1; Fig. S1). V_{cmax} and A_{max} are comparable in this species: *C. merolae*'s rubisco V_{cmax} was measured in cell extracts (see below) as 27 pmol µg Chl a^{-1} s^{-1} at 25 °C, which is comparable to the cellular A_{max} of approximately 20 to 60 pmol µg Chl a^{-1} s^{-1} (in Fig. S1, 35 pmol µg Chl a^{-1} s^{-1} at 40 °C and 25 pmol µg Chl a^{-1} s^{-1} at 30 °C). *C. merolae*'s A_{max} and V_{cmax} are additionally comparable to A_{max} values of three green microalgae, which range from 0.90 to 1.8 pg C pg Chl a^{-1} h^{-1} (21 to 42 pmol µg Chl a^{-1} s^{-1}) (Hupp et al. 2021).

The oxygen-response slope of the compensation point is also of interest as a physiological response influenced by the CCM, and can be extracted by fitting a linear trendline to compensation point predictions at various O_2 concentrations. We additionally made comparisons to Γ_{CO_2} data on the model alga *Chlamydomonas reinhardtii*, which operates a robust and well-characterized CCM (Mackinder 2017). Comparisons to *C. reinhardtii* were made by digitizing the compensation point data of Coleman and Colman (1980) with the WebPlotDigitizer application (v4.5, https://automeris.io/WebPlotDigitizer/). Following an ideal-gas-based

unit conversion of the data on oxygen and temperature response of *C. reinhardtii*, we applied a linear regression to fit the data and used this regression to calculate the compensation point under conditions of interest. This digitizer application was also used to digitize some literature $\delta^{13}C$ and A_{max} values.

Dissolved Ci modeling

The R package "seacarb" (v2.1.12, Lavigne et al. (2019)) was used to calculate dissolved Ci concentrations under various environmental conditions.

Rubisco activity assay

Dense cell cultures (OD_{750} ~ 2, ~ 50 mL) were concentrated (300 × *g*, 25 min) into 1 mL samples. These cell samples were washed (300 × *g*, 10 min) in growth media prepared at pH 7, and cell pellets were then placed at − 20 °C overnight. The pellets were then thawed in 1 mL extraction buffer (pH 8.1, 50 mM 3-[4-(2-Hydroxyethyl)piperazin-1-yl]propane-1-sulfonic acid (EPPS) buffer, 1% w/v polyvinyl polypyrrolidone, 1 mM ethylenediaminetetraacetic acid, 10 mM dithiothreitol, 0.1% Triton surfactant), then spun down (18,407 × *g*, 5 min) to remove cell debris and undissolved polyvinyl polypyrrolidone. To determine chlorophyll content for normalization of rubisco activity, 10 µL of extract was added to 990 µL methanol, and chlorophyll content was spectrophotometrically determined as described above.

To determine rubisco activity, the extract was tested by a spectrophotometric assay coupling reduced nicotinamide adenine dinucleotide (NADH) consumption to RuBP carboxylation, in a manner similar to the methods of Singh et al. (2022) and Kubien et al. (2010). The reaction was initiated by adding 10–80 µL extract and then 50 mM RuBP to a cuvette containing assay buffer (pH 8.0, 50 mM 2-[4-(2-Hydroxyethyl)piperazin-1-yl]ethane-1-sulfonic acid and sodium hydroxide (HEPES–NaOH) buffer, 20 mM magnesium chloride, 1 mM ethylenediaminetetraacetic acid, 1 mM adenosine triphosphate, 5 mM coupling enzyme cocktail, 20 mM sodium bicarbonate, 0.2 mM NADH). The coupling enzyme cocktail contained 20 units glyceraldehyde-3-phosphate dehydrogenase, 22.5 units 3-phosphoglyceric phosphokinase, 12.5 units creatine phosphokinase, 250 units carbonic anhydrase, and 56 units triose-phosphate isomerase. The rubisco carboxylation rate V_{cmax} was determined by monitoring the rate of RuBP-dependent NADH consumption at 340 nm and using NADH extinction coefficient 6.22 Abs_{340} $mmol^{-1}$ cm^{-1} and carboxylation:NADH consumption stoichiometry of 1:4.

Carbon isotope analysis

A gas analyzer (Aerodyne Research, Inc.) was used to determine $\delta^{13}C$ of the ambient air with Tunable Infrared Laser Direct Absorption Spectroscopy. Raw gas analyzer output was corrected based on a calibration gas mixture of known isotopologues mixing ratio (Airgas, Inc.). Algae samples (OD_{750} 1.1, ~ 12 mL) were loaded into glass vials and freeze-dried in a FreeZone 12 lyophilizer (Labconco Corporation) at − 45 °C for approximately 27 h. The dried samples were ground into a fine powder and submitted for $\delta^{13}C$ analysis to Lindsey Conaway and Erik Pollock (University of Arkansas Stable Isotope Laboratory). Biomass samples of approximately 0.3 mg were encapsulated in tin and analyzed on an EA-isolink elemental analyzer interfaced via ConFlo IV to a Delta V plus isotope ratio mass spectrometer (Thermo Electron Bermen). Raw measurements were normalized to international scale values using two reference materials: USGS41a ($n = 3$, standard $\delta^{13}C = 36.55$ ‰, measured $\delta^{13}C = 36.55 \pm 0.03$ ‰ [mean ± S.D.]) and USGS8573 ($n = 3$, standard $\delta^{13}C = -26.39$ ‰, measured $\delta^{13}C = -26.39 \pm 0.09$ ‰ [mean ± S.D.]).

Identification of homologs to known CCM components

To identify *C. merolae* loci potentially involved in a carbon-concentrating mechanism, we used the BLASTX service of the *Cyanidioschyzon merolae* Genome Project (v3, http://czon.jp/blast/blast_cs.cgi). Queries were translated sequences of genes implicated in Ci accumulation by *C. reinhardtii,* bacteria, or diatoms (see Table S1 for a list of literature on these genes, which were sourced from Atkinson et al. (2015), Badger et al. (2002), Klanchui et al. (2017), Mackinder et al. (2017), Matsuda et al. (2017), Mukherjee et al. (2019), and Price et al. (2004)). BLASTP on the NCBI server (https://blast.ncbi.nlm.nih.gov/Blast.cgi) was used to determine whether apparent homologous proteins were reciprocal best hits. Subcellular localization of *C. merolae* loci was predicted with TargetP (Emanuelsson et al. 2000) and with PredAlgo when available (Tardif et al. 2012). Transcriptional data for *C. merolae* genes was sourced from Rademacher et al. (2017).

Supplementary Information The online version contains supplementary material available at https://doi.org/10.1007/s11120-023-01000-6.

Acknowledgements The authors are grateful to Luke Gregory for making the ambient air $\delta^{13}C$ measurement which appears in this paper, to the University of Arkansas Stable Isotope Laboratory for biomass $\delta^{13}C$ analysis, to Dr. Peter Lammers for providing the *C. merolae* cells used to start our cultures, to Audrey Johnson for synthesizing the ribulose 1,5-bisphosphate used in our rubisco activity assay, and to Ludmila Roze for preparing the coupling enzyme cocktail used in our rubisco activity assay. We additionally thank Joshua Kaste, Dr. Danielle

Hoffmann, Antwan Green, and the anonymous peer reviewers for helpful feedback. Furthermore, we extend our gratitude to the attendees of the 10th International Symposium on Inorganic Carbon Utilization in Aquatic Photosynthetic Organisms, whose insights helped to develop our work. We gratefully acknowledge financial support from the Michigan State University College of Natural Science, from the National Institute of General Medical Sciences of the National Institutes of Health, and from the United States Department of Energy.

Author contributions All authors contributed to the study conception and design. Material preparation, data collection and analysis were performed by AKS, except where otherwise noted in the Acknowledgements. The first draft of the manuscript was written by AKS, and all authors commented on previous versions of the manuscript. All authors read and approved the final manuscript.

Funding The work described was supported by a predoctoral training award to AKS from grant number T32-GM110523 from the National Institute of General Medical Sciences of the National Institutes of Health. AKS also received fellowship support from the Michigan State University College of Natural Science and travel support from the Michigan State University-Department of Energy Plant Research Laboratory. Work in the laboratory of YSH is supported by Grant Number DE-SC0018269 from the United States Department of Energy, and BJW was funded by the Division of Chemical Sciences, Geosciences and Biosciences, Office of Basic Energy Sciences of the United States Department of Energy (Grant Number DE-FG02-91ER20021). The contents of this publication are solely the responsibility of the authors and do not necessarily represent the official views of the National Institute of General Medical Sciences, the National Institutes of Health, Michigan Statement University, or the Department of Energy.

Data and code availability The data and code have not been deposited in a public repository, but are available upon request through the corresponding author.

Declarations

Competing interests The authors have no other relevant financial or non-financial interests to disclose.

Research involving human and animals rights Not applicable.

Ethical approval Not applicable.

Informed consent Not applicable.

References

Albertano P, Ciniglia C, Pinto G, Pollio A (2000) The taxonomic position of *Cyanidium*, *Cyanidioschyzon* and *Galdieria*: an update. Hydrobiologia 433:137–143. https://doi.org/10.1023/A:1004031123806

Atkinson N, Feike D, Mackinder LCM, Meyer MT, Griffiths H, Jonikas MC, Smith AM, McCormick AJ (2015) Introducing an algal carbon-concentrating mechanism into higher plants: location and incorporation of key components. Plant Biotechnol J 14:1302–1315. https://doi.org/10.1111/pbi.12497

Badger MR, Kaplan A, Berry JA (1980) Internal inorganic carbon pool of *Chlamydomonas reinhardtii*: evidence for a carbon dioxide-concentrating mechanism. Plant Physiol 66:407–413. https://doi.org/10.1104/pp.66.3.407

Badger MR, Andrews TJ, Whitney SM, Ludwig M, Yellowlees DC, Leggat W, Price GD (1998) The diversity and coevolution of Rubisco, plastids, pyrenoids and chloroplast-based CO_2-concentrating mechanisms in the algae. Can J Bot 76:1052–1071. https://doi.org/10.1139/b98-074

Badger MR, Hanson D, Price GD (2002) Evolution and diversity of CO_2 concentrating mechanisms in cyanobacteria. Funct Plant Biol 29:161–173. https://doi.org/10.1071/PP01213

Barbier G, Oesterhelt C, Larson MD, Halgren RG, Wilkerson C, Garavito RM, Benning C, Weber APM (2005) Comparative genomics of two closely related unicellular thermo-acidophilic red algae, *Galdieria sulphuraria* and *Cyanidioschyzon merolae*, reveals the molecular basis of the metabolic flexibility of *Galdieria sulphuraria* and significant differences in carbohydrate metabolism of both algae. Plant Physiol 137:460–474. https://doi.org/10.1104/pp.104.051169

Barrett J, Girr P, Mackinder LCM (2021) Pyrenoids: CO_2-fixing phase separated liquid organelles. Biochim Biophys Acta - Mol Cell Res. https://doi.org/10.1016/j.bbamcr.2021.118949

Broadwater ST, Scott JL (1994) Ultrastructure of unicellular red algae. In: Seckbach J (ed) Evolutionary pathways and enigmatic algae: *Cyanidium caldarium* (Rhodophyta) and related cells developments in Hydrobiology. Springer, Dordrecht, pp 215–230

Chiodini G, Calrio S, Avino R, Bini G, Guidicepietro F, De Cesare W, Ricciolino P, Aiuppa A, Cardellini C, Petrillo Z, Selva J, Siniscalchi A, Tripaldi S (2021) Hydrothermal pressure-temperature control on CO_2 emissions and seismicity at Campi Flegrei (Italy). J Volcanol Geotherm Res. https://doi.org/10.1016/j.jvolgeores.2021.107245

Coleman JR, Colman B (1980) Effect of oxygen and temperature on the efficiency of photosynthetic carbon assimilation in two microscopic algae. Plant Physiol 65:980–983. https://doi.org/10.1104/pp.65.5.980s

Cummins PL, Kannappan B, Gready JE (2018) Directions for optimization of photosynthetic carbon fixation: RuBisCO's efficiency may not be so constrained after all. Front Plant Sci. https://doi.org/10.3389/fpls.2018.00183

Cunningham FX Jr, Lee H, Gantt E (2007) Carotenoid biosynthesis in the primitive red alga *Cyanidioschyzon merolae*. Eukaryot Cell 6:533–545. https://doi.org/10.1128/EC.00265-06

Curien G, Lyska D, Guglielmino E, Westhoff P, Janetzko J, Tardif M, Hallopeau C, Brugière S, Dal Bo D, Decelle J, Gallet B, Falconet D, Carone M, Remacle C, Ferro M, Weber APM, Finazzi G (2021) Mixotrophic growth of the extremophile *Galdieria sulphuraria* reveals the flexibility of its carbon assimilation metabolism. New Phytol 231:326–338. https://doi.org/10.1111/nph.17359

De Luca P, Taddei R, Varano L (1978) « *Cyanidioschyzon merolae* »: a new alga of thermal acidic environments. Webbia 33:37–44. https://doi.org/10.1080/00837792.1978.10670110

di Cicco MR, Iovinella M, Palmieri M, Lubritto C, Ciniglia C (2021) Extremophilic microalgae galdieria Gen. for urban wastewater treatment: current state, the case of "POWER" system, and future prospects. Plants. https://doi.org/10.3390/plants10112343

Edwards GE, Franceschi VR, Voznesenskaya EV (2004) Single-cell C_4 photosynthesis versus the dual-cell (Kranz) paradigm. Annu Rev Plant Biol 55:173–196. https://doi.org/10.1146/annurev.arplant.55.031903.141725

Emanuelsson O, Nielsen H, Brunak S, von Heijne G (2000) Predicting subcellular localization of proteins based on their N-terminal amino acid sequence. J Mol Biol 300:1005–1016. https://doi.org/10.1006/jmbi.2000.3903

Fei C, Wilson AT, Mangan NM, Wingreen NS, Jonikas MC (2022) Modelling the pyrenoid-based CO_2-concentrating mechanism provides insights into its operating principles and a roadmap for its engineering into crops. Nat Plants 8:583–595. https://doi.org/10.1038/s41477-022-01153-7

Fierro P Jr (2007) Constants and conversion factors. In: Fierro P Jr, Nyer EK (eds) The water encyclopedia: hydrologic data and internet resources, 3rd edn. CRC Press, Boca Raton, pp 13-12–13-19

Flamholz AI, Prywes N, Moran U, Davidi D, Bar-On YM, Oltrogge LM, Alves R, Savage D, Milo R (2019) Revisiting trade-offs between Rubisco kinetic parameters. Biochem 58:3365–3376. https://doi.org/10.1021/acs.biochem.9b00237

Fujiwara T, Hirooka S, Mukai M, Ohbayashi R, Kanesaki Y, Wananabe S, Miyagishima S-y (2019) Integration of a *Galdieria* plasma membrane sugar transporter enables heterotrophic growth of the obligate photoautotrophic red alga *Cynanidioschyzon merolae*. Plant Direct. https://doi.org/10.1002/pld3.134

Galmés J, Hermida-Carrera C, Laanisto L, Niinemets Ü (2016) A compendium of temperature responses of Rubisco kinetic traits: variability among and within photosynthetic groups and impacts on photosynthesis modeling. J Exp Bot. https://doi.org/10.1093/jxb/erw267

Gehl KA, Colman B (1985) Effect of external pH on the internal pH of *Chlorella saccharophila*. Plant Physiol 77:917–921. https://doi.org/10.1104/pp.77.4.917

Giordano M, Beardall J, Raven JA (2005) CO_2 Concentrating mechanisms in algae: mechanisms, environmental modulation, and evolution. Annu Rev Plant Biol 56:99–131. https://doi.org/10.1146/annurev.arplant.56.032604.144052

Goudet MMM, Orr DJ, Melkonian M, Müller KH, Meyer MT, Carmo-Silva E, Griffiths H (2020) Rubisco and carbon-concentrating mechanism co-evolution across chlorophyte and streptophyte green algae. New Phytol 227:810–823. https://doi.org/10.1111/nph.16577

Griffiths H, Meyer MT, Rickaby REM (2017) Overcoming adversity through diversity: aquatic carbon concentrating mechanisms. J Exp Bot 68:3689–3695. https://doi.org/10.1093/jxb/erx278

Gross W (2000) Ecophysiology of algae living in highly acidic environments. Hydrobiologia 433:31–37. https://doi.org/10.1023/A:1004054317446

Hagemann M, Kern R, Maurino VG, Hanson DT, Weber APM, Sage RF, Bauwe H (2016) Evolution of photorespiration from cyanobacteria to land plants, considering protein phylogenies and acquisition of carbon concentrating mechanisms. J Exp Bot 67:2963–2976. https://doi.org/10.1093/jxb/erw063

Hennacy JH, Jonikas MC (2020) Prospects for engineering biophysical CO_2 concentrating mechanisms into land plants to enhance yields. Annu Rev Plant Biol 71:461–485. https://doi.org/10.1146/annurev-arplant-081519-040100

Hopkinson BM, Dupont CL, Matsuda Y (2016) The physiology and genetics of CO_2 concentrating mechanisms in model diatoms. Curr Opin Plant Biol 31:51–57. https://doi.org/10.1016/j.pbi.2016.03.013

Hupp J, McCoy JIE, Millgan AJ, Peers G (2021) Simultaneously measuring carbon uptake capacity and chlorophyll *a* fluorescence dynamics in algae. Algal Res. https://doi.org/10.1016/j.algal.2021.102399

Hurley SJ, Wing BA, Jasper CE, Hill NC (2021) Carbon isotope evidence for the global physiology of proterozoic cyanobacteria. Sci Adv. https://doi.org/10.1126/sciadv.abc8998

Ichinose TM, Iwane AH (2017) Cyotological analyses by advanced electron microscopy. In: Kuroiwa T, Miyagishima S, Matsunaga S et al (eds) *Cyanidioschyzon merolae*: a new model eukaryote for cell and organelle biology. Springer, Singapore, pp 129–152

Im CS, Grossman AR (2002) Identification and regulation of high light-induced genes in *Chlamydomonas reinhardtii*. Plant J 30:301–313. https://doi.org/10.1046/j.1365-313X.2001.01287.x

Imoto Y, Yoshida Y (2017) Cellular structure of *Cyanidioschyzon merolae*: a minimum set of organelles. In: Kuroiwa T, Miyagishima S, Matsunaga S et al (eds) *Cyanidioschyzon merolae*: a new model eukaryote for cell and organelle biology. Springer, Singapore, pp 17–30. https://doi.org/10.1007/978-981-10-6101-1

Iñiguez C, Capó-Bauça S, Niinemets Ü, Stoll H (2020) Evolutionary trends in RuBisCO kinetics and their co-evolution with CO_2 concentrating mechanisms. Plant J 101:897–918. https://doi.org/10.1111/tpj.14643

Jensen EL, Maberly SC, Gontero B (2020) Insights on the functions and ecophysiological relevance of the diverse carbonic anhydrases in microalgae. Int J Mol Sci. https://doi.org/10.3390/ijms21082922

Klanchui A, Cheevadhanarak S, Prommeenate P, Meechai A (2017) Exploring components of the CO_2-concentrating mechanism in alkaliphilic cyanobacteria through genome-based analysis. Comput Struct Biotechnol J 15:340–350. https://doi.org/10.1016/j.csbj.2017.05.001

Kohn MJ (2010) Carbon isotope compositions of terrestrial C3 plants as indicators of (paleo)ecology and (paleo)climate. Proc Natl Acad Sci USA 107:19691–19695. https://doi.org/10.1073/pnas.1004933107

Kramer DM, Sacksteder CA, Cruz JA (1999) How acidic is the lumen? Photosynth Res 60:151–163. https://doi.org/10.1023/A:1006212014787

Kubien DS, Brown CM, Kane HJ (2010) Quantifying the amount and activity of rubisco in leaves. In: Carpentier R (ed) Photosynthesis research protocols. Methods in molecular biology, vol 684. Humana Press, Totowa, pp 349–362

Kuroiwa T, Miyagishima S, Matsunaga S (2017) Preface. In: Kuroiwa T, Miyagishima S, Matsunaga S et al (eds) *Cyanidioschyzon merolae*: a new model eukaryote for cell and organelle biology. Springer, Singapore, pp 5–7. https://doi.org/10.1007/978-981-10-6101-1

Lang I, Bashir S, Lorenz M, Rader S, Weber G (2020) Exploiting the potential of Cyanidiales as a valuable resource for biotechnological applications. Appl Phycol. https://doi.org/10.1080/26388081.2020.1765702

Lavigne H, Proye A, Gattuso JP (2019) Seacarb: calculates parameters of the seawater carbonate system. 2.1.2 edn

Liu SL, Chiang YR, Yoon HS, Fu HY (2020) Comparative genome analysis reveals *Cyanidiococcus gen. nov.*, A new Extremophilic red algal genus sister to *Cyanidioschyzon* (Cyanidioschyzonaceae, Rhodophyta). J Phycol 56:1429–1442. https://doi.org/10.1111/jpy.13056

Loganathan N, Tsai YCC (2016) Characterization of the heterooligomeric red-type rubisco activase from red algae. PNAS 113:14019–14024. https://doi.org/10.1073/pnas.1610758113

Mackinder LCM (2017) The *Chlamydomonas* CO_2-concentrating mechanism and its potential for engineering photosynthesis in plants. New Phytol 217:54–61. https://doi.org/10.1111/nph.14749

Mackinder LCM, Chen C, Leib RD, Patena W, Blum SR, Rodman M, Ramundo S, Adams CM, Jonikas MC (2017) A spatial interactome reveals the protein organization of the algal CO_2-concentrating mechanism. Cell 171:133–147. https://doi.org/10.1016/j.cell.2017.08.044

Mangan NM, Flamholz A, Hood RD, Milo R, Savage DF (2016) pH determines the energetic efficiency of the cyanobacterial CO_2 concentrating mechanism. PNAS 113:E5354–E5362. https://doi.org/10.1073/pnas.1525145113

Marino D, Cañas RA, Betti M (2022) Is plastidic glutamine synthetase essential for C_3 plants? A tale of photorespiratory mutants, ammonium tolerance and conifers. New Phytol 234:1559–1565. https://doi.org/10.1111/nph.18090

Matsuda Y, Hopkinson BM, Nakajima K, Dupont CL, Tsuji Y (2017) Mechanisms of carbon dioxide acquisition and CO_2 sensing in marine diatoms: a gateway to carbon metabolism. Philos Trans R Soc Lond B Biol Sci. https://doi.org/10.1098/rstb.2016.0403

Matsuzaki M, Misumi O, Shin-i T, Maruyama S, Takahara M, Miyagishima S-y, Mori T, Nishida K, Yagisawa F, Nishida K, Yoshida Y, Nishimura Y, Nakao S, Kobayashi T, Momoyama Y, Higashiyama T, Minoda A, Sano M, Nomoto H, Oishi K, Hayashi H, Ohta F, Nishizaka S, Haga S, Miura S, Morishita T, Kabeya Y, Terasawa K, Suzuki Y, Ishii Y, Asakawa S, Takano H, Ohta N, Kuroiwa H, Tanaka K, Shimizu N, Sugano S, Sato N, Nozaki H, Ogasawara N, Kohara Y, Kuroiwa T (2004) Genome sequence of the ultrasmall unicellular red alga *Cyanidioschyzon merolae* 10D. Nature 428:653–657. https://doi.org/10.1038/nature02398

McGrath JM, Long SP (2014) Can the cyanobacterial carbon-concentrating mechanism increase photosynthesis in crop species? A theoretical analysis. Plant Physiol 164:2247–2261. https://doi.org/10.1104/pp.113.232611

Meyer M, Griffiths H (2013) Origins and diversity of eukaryotic CO_2-concentrating mechanisms: lessons for the future. J Exp Bot 64:769–786. https://doi.org/10.1093/jxb/ers390

Meyer MT, McCormick AJ, Griffiths H (2016) Will an algal CO_2-concentrating mechanism work in higher plants? Curr Opin Plant Biol 31:181–188. https://doi.org/10.1016/j.pbi.2016.04.009

Meyer MT, Whittaker C, Griffiths H (2017) The algal pyrenoid: key unanswered questions. J Exp Bot 68:3739–3749. https://doi.org/10.1093/jxb/erx178

Minoda A, Sakagami R, Yagisawa F, Kuroiwa T, Tanaka K (2004) Improvement of culture conditions and evidence for nuclear transformation by homologous recombination in a red alga, *Cyanidioschyzon merolae* 10D. Plant Cell Physiol 45:667–671. https://doi.org/10.1093/pcp/pch087

Misumi O, Matsuzaki M, Nozaki H, Miyagishima S-y, Mori T, Nishida K, Yagisawa F, Yoshida Y, Kuroiwa H, Kuroiwa H (2005) *Cyanidioschyzon merolae* genome. A tool for facilitating comparable studies on organelle biogenesis in photosynthetic eukaryotes. Plant Physiol 137:567–585. https://doi.org/10.1104/pp.104.053991

Misumi O, Kuroiwa T, Hirooka S (2017) Application of the tolerance to extreme environment to land plants. In: Kuroiwa T, Miyagishima S, Matsunaga S et al (eds) *Cyanidioschyzon merolae*: a new model eukaryote for cell and organelle biology. Springer, Singapore, pp 325–341. https://doi.org/10.1007/978-981-10-6101-1

Mitchell MC, Meyer MT, Griffiths H (2014) Dynamics of carbon-concentrating mechanism induction and protein relocalization during the dark-to-light transition in synchronized *Chlamydomonas reinhardtii*. Plant Physiol 166:1073–1082. https://doi.org/10.1104/pp.114.246918

Miyagishima S, Wei JL (2017) Procedures for cultivation, observation, and conventional experiments in *Cyanidioschyzon merolae*. In: Kuroiwa T, Miyagishima S, Matsunaga S et al (eds) *Cyanidioschyzon merolae*: a new model eukaryote for cell and organelle biology. Springer, Singapore, pp 31–42. https://doi.org/10.1007/978-981-10-6101-1

Miyagishima S, Wei JL, Nozaki H, Hirooka S (2017) Cyanidiales: evolution and habitats. In: Kuroiwa T, Miyagishima S, Matsunaga S et al (eds) *Cyanidioschyzon merolae*: a new model eukaryote for cell and organelle biology. Springer, Singapore, pp 3–16. https://doi.org/10.1007/978-981-10-6101-1

Mori N, Moriyama T, Toyoshima M, Sato N (2016) Construction of global acyl lipid metabolic map by comparative genomics and subcellular localization analysis in the red alga *Cyanidioschyzon merolae*. Front Plant Sci. https://doi.org/10.3389/fpls.2016.00958

Morita E, Abe T, Tsuzuki M, Fujiwara S, Sato N, Hirata A, Sonoike K, Nozaki H (1998) Presence of the CO_2-concentrating mechanism in some species of the pyrenoid-less free-living algal genus *Chloromonas* (Volvocales, Chlorophyta). Planta 204:269–276. https://doi.org/10.1007/s004250050256

Moriyama T, Sakurai K, Sekine K, Sato N (2014) Subcellular distribution of central carbohydrate metabolism pathways in the red alga *Cyanidioschyzon merolae*. Planta 240:585–598. https://doi.org/10.1007/s00425-014-2108-0

Moriyama T, Mori N, Sato N (2015) Activation of oxidative carbon metabolism by nutritional enrichment by photosynthesis and exogenous organic compounds in the red alga *Cyanidioschyzon merolae*: evidence for heterotrophic growth. Springerplus. https://doi.org/10.1186/s40064-015-1365-0

Moriyama T, Mori N, Sato N (2017) Carbon Metabolism. In: Kuroiwa T, Miyagishima S, Matsunaga S et al (eds) *Cyanidioschyzon merolae*: a new model eukaryote for cell and organelle biology. Springer, Singapore, pp 297–321. https://doi.org/10.1007/978-981-10-6101-1

Moriyama T, Mori N, Nagata N, Sato N (2018) Selective loss of photosystem I and formation of tubular thylakoids in heterotrophically grown red alga *Cyanidioschyzon merolae*. Photosynth Res 140:275–287. https://doi.org/10.1007/s11120-018-0603-z

Moroney JV, Bartlett SG, Samuelsson G (2004) Carbonic anhydrases in plants and algae. Plant Cell Environ 24:141–153. https://doi.org/10.1111/j.1365-3040.2001.00669.x

Moroney JV, Ma Y, Frey WD, Fusilier KA, Pham TT, Simms TA, DiMario RJ, Yang J, Mukherjee B (2011) The carbonic anhydrase isoforms of *Chlamydomonas reinhardtii*: intracellular location, expression, and physiological roles. Photosynth Res 109:133–149. https://doi.org/10.1007/s11120-011-9635-3

Moroney JV, Jungnick N, DiMario RJ, Longstreth DJ (2013) Photorespiration and carbon concentrating mechanisms: two adaptations to high O_2, low CO_2 conditions. Photosynth Res 117:121–131. https://doi.org/10.1007/s11120-013-9865-7

Mukherjee A, Lau CS, Walker CE, Rai AK, Prejean CI, Yates G, Emrich-Mills T, Lemoine SG, Vinyard DJ, Mackinder LCM, Moroney JV (2019) Thylakoid localized bestrophin-like proteins are essential for the CO_2 concentrating mechanism of *Chlamydomonas reinhardtii*. PNAS 116:16915–16920. https://doi.org/10.1073/pnas.1909706111

Neofotis P, Temple J, Tessmer OL, Bibik J, Norris N, Pollner E, Lucker B, Weaduwage SM, Withrow A, Sears B, Mogos G, Frame M, Hall D, Weissman J, Kramer DM (2021) The induction of pyrenoid synthesis by hyperoxia and its implications for the natural diversity of photosynthetic responses in *Chlamydomonas*. Elife. https://doi.org/10.7554/eLife.67565

O'Leary MH (1988) Carbon Isotopes in Photosynthesis: fractionation techniques may reveal new aspects of carbon dynamics in plants. Bioscience 38:328–336. https://doi.org/10.2307/1310735

Oesterhelt C, Schmälzlin E, Schmitt JM, Lokstein H (2007) Regulation of photosynthesis in the unicellular acidophilic red alga *Galdieria sulphuraria*. Plant J 51:500–511. https://doi.org/10.1111/j.1365-313X.2007.03159.x

Parys E, Krupnik T, Kulak I, Kania K, Romanowska E (2021) Photosynthesis of the *Cyanidioschyzon merolae* cells in blue, red, and white light. Photosynth Res 147:61–73. https://doi.org/10.1007/s11120-020-00796-x

Price GD, Badger MR (1989) Expression of human carbonic anhydrase in the Cyanobacterium *Synechococcus* PCC7942 creates a high CO_2-requiring phenotype: evidence for a central role for carboxysomes in the CO_2 concentrating mechanism. Plant Physiol 91:505–513. https://doi.org/10.1104/pp.91.2.505

Price GD, Woodger FJ, Badger MR, Howitt SM, Tucker L (2004) Identification of a SulP-type bicarbonate transporter in marine cyanobacteria. PNAS 101:18228–18233. https://doi.org/10.1073/pnas.0405211101

Price GD, Badger MR, Woodger FJ, Long BM (2008) Advances in understanding the cyanobacterial CO_2-concentrating-mechanism (CCM): functional components, Ci transporters, diversity, genetic regulation and prospects for engineering into plants. J Exp Bot 59:1441–1461. https://doi.org/10.1093/jxb/erm112

Price GD, Badger MR, von Caemmerer S (2011) The Prospect of using cyanobacterial bicarbonate transporters to improve leaf photosynthesis in C_3 crop plants. Plant Physiol 155:20–26. https://doi.org/10.1104/pp.110.164681

Rademacher N, Kern R, Fujiwara T, Mettler-Altmann MSY, Hagemann M, Eisenhut M, Weber APM (2016) Photorespiratory glycolate oxidase is essential for the survival of the red alga *Cyanidioschyzon merolae* under ambient CO_2 conditions. J Exp Bot 67:3165–3175. https://doi.org/10.1093/jxb/erw118

Rademacher N, Wrobel TJ, Rossoni AW, Kurz S, Bräutigam A, Weber APM, Eisenhut M (2017) Transcriptional response of the extremophile red alga *Cyanidioschyzon merolae* to changes in CO_2 concentrations. J Plant Physiol 217:49–56. https://doi.org/10.1016/j.jplph.2017.06.014

Rae BD, Long BM, Förster B, Nguyen ND, Velanis CN, Atkinson N, Hee WY, Mukherjee B, Price GD, McCormick AJ (2017) Progress and challenges of engineering a biophysical CO_2-concentrating mechanism into higher plants. J Exp Bot 68:3717–3737. https://doi.org/10.1093/jxb/erx133

Raven JA, Beardall J (2003) Carbon acquisition mechanisms of algae: carbon dioxide diffusion and carbon dioxide concentrating mechanisms. In: Larkum AWD, Douglas SE, Raven JA (eds) Photosynthesis in algae, Advances in photosynthesis and respiration, vol 14. Springer, Dordrecht, pp 226–241

Raven JA, Johnston AM, Kübler JE, Korb R, McInroy SG, Handley LL, Scrimgeour CM, Walker DI, Beardall J, Vanderklift M, Fredriksen S, Dunton KH (2002) Mechanistic interpretation of carbon isotope discrimination by marine macroalgae and seagrasses. Funct Plant Biol 29:355–378. https://doi.org/10.1071/PP01201

Raven JA, Cockell CS, De La Rocha CL (2008) The evolution of inorganic carbon concentrating mechanisms in photosynthesis. Philos Trans R Soc Lond B Biol Sci 363:2641–2650. https://doi.org/10.1098/rstb.2008.0020

Raven JA, Ball LA, Beardall J, Giordano M, Maberly SC (2011) Algae lacking CO_2 concentrating mechanisms. Can J Bot 83:879–890. https://doi.org/10.1139/B05-074

Ritchie RJ (2006) Consistent sets of spectrophotometric chlorophyll equations for acetone, methanol and ethanol solvents. Photosynth Res 89:27–41. https://doi.org/10.1007/s11120-006-9065-9

Ritz C, Baty F, Streibig JC, Gerhard D (2015) Dose-response analysis using R. PLoS ONE. https://doi.org/10.1371/journal.pone.0146021

Sage TL, Sage RF, Vogan PJ, Rahman B, Johnson DC, Oakley JC, Heckel MA (2011) The occurrence of C_2 photosynthesis in *Euphorbia* subgenus Chamaesyce (*Euphorbiaceae*). J Exp Bot 62:3183–3195. https://doi.org/10.1093/jxb/err059

Sato N, Moriyama T, Mori N, Toyoshima M (2017) Lipid metabolism and potentials of biofuel and high added-value oil production in red algae. World J Microbiol Biotechnol. https://doi.org/10.1007/s11274-017-2236-3

Sharkey TD, Berry JA (1985) Carbon isotope fractionation of algae as influenced by an inducible CO_2 concentrating mechanism. In: Lucas WJ, Berry JA (eds) Inorganic carbon uptake by aquatic photosynthetic organisms. American Society of Plant Phytologists, Rockville, pp 389–401

Singh AK, Santos-Merino M, Sakkos JK, Walker BJ, Ducat DC (2022) Rubisco regulation in response to altered carbon status in the cyanobacterium *Synechococcus elongatus* PCC 7942. Plant Physiol 189:874–888. https://doi.org/10.1093/plphys/kiac065

Spalding MH, Portis AR Jr (1985) A model of carbon dioxide assimilation in *Chlamydomonas reinhardii*. Planta 164:308–320. https://doi.org/10.1007/BF00402942

Stadnichuk IN, Tropin IV (2022) Cyanidiales as polyextreme eukaryotes. Biochem (Mosc) 87:472–487. https://doi.org/10.1134/S000629792205008X

Takusagawa M, Nakajima Y, Saiyo T, Misumi O (2016) Primitive red alga *Cyanidioschyzon merolae* accumulates storage glucan and triacylglycerol under nitrogen depletion. J Gen Appl Microbiol 62:111–117. https://doi.org/10.2323/jgam.2015.12.001

Tardif M, Atteia A, Specht M, Cogne G, Rolland N, Brugière S, Hippler M, Ferro M, Bruley C, Peltier G, Vallon O, Cournac L (2012) PredAlgo: a new subcellular localization prediction tool dedicated to green algae. Mol Biol Evol 29:3625–3639. https://doi.org/10.1093/molbev/mss178

Tolbert NE, Benker C, Beck E (1995) The oxygen and carbon dioxide compensation points of C_3 plants: possible role in regulating atmospheric oxygen. PNAS 92:11230–11233. https://doi.org/10.1073/pnas.92.24.11230

Toyoshima M, Mori N, Moriyama T, Misumi O, Sato N (2016) Analysis of triacylglycerol accumulation under nitrogen deprivation in the red alga *Cyanidioschyzon merolae*. Microbiology 162:803–812. https://doi.org/10.1099/mic.0.000261

Uemura K, Anwaruzzaman MS, Yokota A (1997) Ribulose-1,5-Bisphosphate Carboxylase/Oxygenase from Thermophilic red algae with a strong specificity for CO_2 fixation. Biochem Biophys Res Commun 233:568–571. https://doi.org/10.1006/bbrc.1997.6497

Vance P, Spalding MH (2005) Growth, photosynthesis, and gene expression in *Chlamydomonas* over a range of CO_2 concentrations and CO_2/O_2 ratios: CO_2 regulates multiple acclimation states. Can J Bot. https://doi.org/10.1139/b05-064

Varshney P, Mikulic P, Vonshak A, Beardall J, Wangikar PP (2015) Extremophilic micro-algae and their potential contribution in biotechnology. Bioresour Technol 184:363–372. https://doi.org/10.1016/j.biortech.2014.11.040

Venturi S, Tassi F, Biococchi G, Cabassi J, Capecchiacii F, Capasso G, Vaseli O, Ricci A, Grassa F (2017) Fractionation processes affecting the stable carbon isotope signature of thermal waters from hydrothermal/volcanic systems: the examples of Campi Flegrei and Vulcano Island (Southern Italy). J Volcanol Geotherm 345:46–57. https://doi.org/10.1016/j.jvolgeores.2017.08.001

Villarejo A, García Reina G, Ramazanov Z (1996) Regulation of the low-CO_2-inducible polypeptides in *Chlamydomonas reinhardtii*. Planta 199:481–485. https://doi.org/10.1007/BF00195176

Vogel JC, Grootes PM, Mook WG (1970) Isotopic fractionation between gaseous and dissolved carbon dioxide. Z Phys A 230:225–238. https://doi.org/10.1007/BF01394688

von Caemmerer S (2000) Biochemical models of leaf photosynthesis. CSIRO Publishing, Collingwood

von Caemmerer S, Edwards GE, Koteteva N, Cousins AB (2014) Single cell C_4 photosynthesis in aquatic and terrestrial plants: a gas

exchange perspective. Aquat Bot 118:71–80. https://doi.org/10.1016/j.aquabot.2014.05.009

Wang Y, Spalding MH (2014) Acclimation to very low CO_2: contribution of limiting CO_2 inducible proteins, LCIB and LCIA, to inorganic carbon uptake in *Chlamydomonas reinhardtii*. Plant Physiol 166:2040–2050. https://doi.org/10.1104/pp.114.248294

Weber APM, Oesterhelt C, Gross W, Bräutigam A, Imboden LA, Krassovskaya I, Linka N, Truchina J, Schneidereit J, Voll H, Voll LM, Zimmermann M, Jamai A, Riekhof WR, Yu B, Garavito RM, Benning C (2004) EST-analysis of the thermo-acidophilic red microalga *Galdieria sulphuraria* reveals potential for lipid A biosynthesis and unveils the pathway of carbon export from rhodoplasts. Plant Mol Biol 55:17–32. https://doi.org/10.1007/s11103-004-0376-y

Weber APM, Horst RJ, Barbier GG, Oesterhelt C (2007) Metabolism and metabolomics of eukaryotes living under extreme conditions. Int Rev Cytol 256:1–34. https://doi.org/10.1016/S0074-7696(07)56001-8

Werdan K, Heldt HW, Milovancev M (1975) The role of pH in the regulation of carbon fixation in the chloroplast stroma. Studies on CO_2 fixation in the light and dark. Biochim Biophys Acta Bioenerg 396:276–292. https://doi.org/10.1016/0005-2728(75)90041-9

Whitney SM, Baldet P, Hudson GS, Andrews TJ (2001) Form I Rubiscos from non-green algae are expressed abundantly but not assembled in tobacco chloroplasts. Plant J 26:535–547. https://doi.org/10.1046/j.1365-313x.2001.01056.x

Wu Y, Xu Y, Li H, Xing D (2012) Effect of acetazolamide on stable carbon isotope fractionation in *Chlamydomonas reinhardtii* and *Chlorella vulgaris*. Chin Sci Bull 57:786–789. https://doi.org/10.1007/s11434-011-4861-9

Wunder T, Oh ZG, Mueller-Cajar O (2019) CO_2-fixing liquid droplets: towards a dissection of the microalgal pyrenoid. Traffic 20:380–389. https://doi.org/10.1111/tra.12650

Young JN, Rickaby REM, Kapralov MV, Filatov DA (2012) Adaptive signals in algal Rubisco reveal a history of ancient atmospheric carbon dioxide. Philos Trans R Soc Lond B Biol Sci 367:483–492. https://doi.org/10.1098/rstb.2011.0145

Young JN, Heureux AMC, Sharwood RE, Rickaby REM, Morel FMM, Whitney SM (2016) Large variation in the Rubisco kinetics of diatoms reveals diversity among their carbon-concentrating mechanisms. J Exp Bot 67:3445–3456. https://doi.org/10.1093/jxb/erw163

Zelitch I, Schultes NP, Peterson RB, Brown P, Brutnell TP (2008) High glycolate oxidase activity is required for survival of maize in normal air. Plant Physiol 149:195–204. https://doi.org/10.1104/pp.108.128439

Zenvirth D, Volokita M, Kaplan A (1985) Photosynthesis and inorganic carbon accumulation in the acidophilic alga *Cyanidioschyzon merolae*. Plant Physiol 77:237–239. https://doi.org/10.1104/pp.77.1.237